Comparison of the global ocean-sea ice experiments in the different grid resolution models

Kim, Cheol-Ho
Korea Institute of Ocean Science and Technology

Jang, Chan Joo
Korea Institute of Ocean Science and Technology

Kim, Minwoo
Korea Institute of Ocean Science and Technology

https://doi.org/10.15017/27138

出版情報：九州大学応用力学研究所所報. 143, pp.63-67, 2012-09. Research Institute for Applied Mechanics, Kyushu University
バージョン：
権利関係：

Comparison of the global ocean-sea ice experiments in the different grid resolution models

Cheol-Ho KIM*1, Chan Joo JANG*1 and Minwoo KIM*1

E-mail of corresponding author: *chkim@kiost.ac*

(Received July 31, 2012)

Abstract

To investigate the changes in the features of the upper ocean with the enhancement of horizontal grid resolution, global ocean circulations are simulated using the two different grid resolution models based on the GFDL ocean-sea ice coupled model, MOM4p1-SIS. The two models use roughly 1 degree x 1 degree (GCM_1) and 0.5 degree x 0.5 degree (GCM_0.5) grid resolution, respectively, except in the equatorial region where more refined grid spacing is taken in meridional direction. Both model employ the common atmospheric data (radiation, wind, air temperature, specific humidity, sea level pressure, precipitation and land runoff) from the CORE-II normal year forcing dataset and adopt the same numerical schemes in tracer and momentum advection and diffusion with the same coefficients of eddy viscosity and eddy diffusivity between them.

After 120 years of integration GCM_1 shows warm biases compared to the observation in the sea surface temperature at the equatorial Western Pacific, Asian Marginal Seas, west off South American coast and several other areas in the Pacific Ocean, including other major areas in the Atlantic, Indian and Southern Oceans. It also shows cold biases at those areas such as the central part of the subtropical gyre in the North Pacific and most of the North Atlantic and Greenland Sea. Compared to GCM_1 GCM_0.5 reveals some improved SST patterns showing much reduced warm- and cold-biased regions at the above mentioned areas. In the surface heat flux distributions GCM_0.5 is shown to receive more heat compared to GCM_1 at those regions close to the continents such as west off north and south American coast, western African coast, and Indo-Pacific Archipelago area.. However, GCM_0.5 loses more heat to the atmosphere at some places such as the Kuroshio extension and the subtropical region in case of North Pacific Ocean.

It is suggested that the improved global surface temperature pattern obtained in GCM_0.5 is much indebted to the strengthening of coastal currents and more refined western boundary currents together with more realistic simulation of meso-scale eddies in the ocean basins due to the enhanced horizontal grid resolution.

Key words : *Global coupled ocean-sea ice model, Grid resolution,, Sea surface temperature, Surface heat flux*

1. Introduction

Global coupled ocean-sea ice model is more useful to express air-sea heat exchanges properly compared to ocean-only circulation model and helps to understand the climate dynamics. Moreover, coupled ocean-sea ice model consists of an important component to climate system model for simulating ocean climate change and/or predicting the sea level rise due to global warming. Yet the state of the art is that the horizontal resolutions adopted in most of the global ocean-sea ice models employed in climate simulations are relatively low and not enough to represent the meso-scale eddies in the oceans and regional oceanic features. It is because of the high computational costs to get the oceanic steady states reaching only after a long-term integration of several hundred years in climate simulation and the increasing number of ensemble runs in climate change experiments. In recent years, however, the enhancement of model resolution is more required as model communities pay more attention to the response of the regional seas in relation to global climate change.

In general, global ocean circulation models with one degree horizontal grid resolution can afford to simulate the western boundary currents and gyre scale circulations in ocean basins, but are not sufficient to

*1 Korea Institute of Ocean Science & Technology

resolve the currents along continental coasts and over continental shelves[1]. Compared to one degree grid resolution global ocean models, 0.2~0.5 degree grid resolution models are shown to simulate the behavior of meso-scale eddies and the coastal currents in more detail [2),3),4),5)]. However, the differences between the simulations with different grid resolution are not known well yet in the global coupled ocean-sea ice models. In this study we consider the some changes in the simulations of the global coupled ocean-sea ice model experiments in relation with the enhancement of grid resolution; roughly one degree and 0.5 degree grid spacing, respectively, in the horizontal direction.

2. Global coupled ocean-sea ice model configuration

The model used in this study is the ocean-sea ice component of the GFDL climate model, MOM4p1-SIS (Modular Ocean Model version 4.1-Sea Ice Simulator[6]). The first global ocean-sea ice model (hereafter GCM_1) is relatively coarse with grid resolution of one degree both in longitudinal and latitudinal direction except in the equatorial region where meridional grid spacing decreases gradually up to 1/3 degree between the equator and 30° N/S to resolve the complex equatorial current system. The second global ocean-sea ice model (hereafter GCM_0.5) has relatively high resolution compared to GCM_1; 0.5 degree grid spacing in longitudinal and latitudinal direction with refined grid spacing in the equatorial region (decreasing from 0.5 degree at 10° N/S to 1/3 degree at the equator). These two models are composed of 50 cells in the vertical with partial step bottom topography. So the GCM_0.5 uses about 4-times more horizontal grid points than the GCM_1 and realizes the global bottom topography more realistically.

Both models adopt the same numerical schemes and parameterizations in tracer and momentum advection and diffusion with the same coefficients of eddy viscosity and eddy diffusivity between them. The major numerical schemes are mdppm for temperature and mdfl_sweby for salinity in the horizontal tracer advection, GM-neutral mixing for the horizontal diffusion, biharmonic friction for momentum diffusion, kpp for vertical mixing, and Bryan-Lewis mixing for background vertical mixing. In addition, pressure-coordinate is used for the vertical grid based on the non-boussinesq equation (mass conservation equation) to simulate the sea level height variation due to the density change. Temperature and salinity from the World Ocean Atlas 98[7] are given for the initial value of the ocean interior. Coordinated Ocean-ice Reference Experiments normal year forcing dataset (CORE-NYF.v2) are used as the surface boundary conditions[6]. CORE-NYF.v2 is a climatological forcing dataset processed at NCAR[8),9)]. The climatological sea surface temperature (SST) in the CORE-NYF.v2 is based on Hadley Center sea Ice and SST (HadISST) data merged with Reynolds SST[10)], and ice concentration from the National Snow and Ice Data Center (NSIDC). Atmospheric variables are composed of radiation, wind, air temperature, specific humidity, sea level pressure, precipitation and continental runoff based on NCEP reanalysis and from other various products. Using bulk formula provided by NCAR and CORE dataset global heat and fresh water flux climatologies were presented by Large and Yeager[8),9)]. However, surface heat fluxes in the model are estimated by the prognostic SST with bulk formula and CORE-NYF.v2 meteorological forcing variables, they are different from the climatological heat fluxes presented by Large and Yeager[9)]. In addition to the surface thermal forcing, surface salinity is restored to the Levitus climatology with the time constant of 60 days to avoid the unrealistic freshening of arctic surface layer by the sea ice melting.

3. Results

We integrated GCM_1 for 1000 years and GCM_0.5 for 120 years using supercomputer. After several decades of integration surface temperature and salinity in GCM_1 and GCM_0.5 show almost steady states in their distribution pattern. The simulated fields at 120 years of integration are used for the analysis.

• Global distribution of surface temperature

Climatological CORE SST is used for the comparison of model and observation because the meteorological forcing variables provided by the CORE dataset and the bulk formula are adjusted for the climatological CORE heat and fresh water flux to be balanced globally.

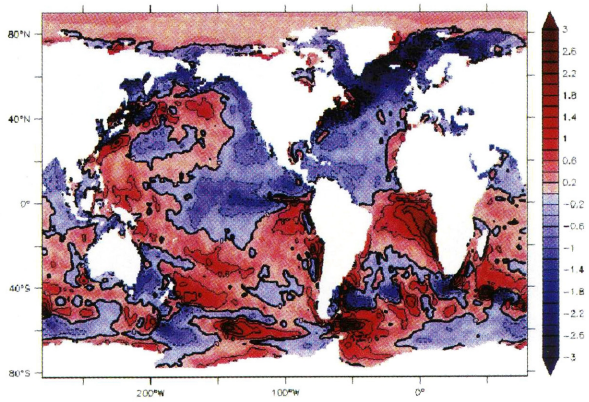

Fig. 1 Difference between the annual mean SST of GCM_1 and SST climatology (GCM_1 minus observation)

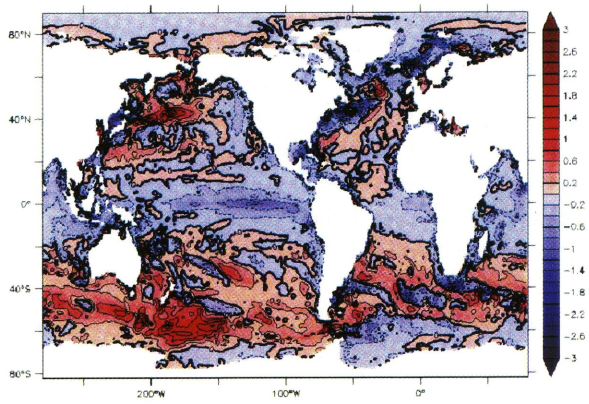

Fig. 2 Difference of the annual mean SST between GCM_0.5 and GCM_1 (GCM_0.5 minus GCM_1)

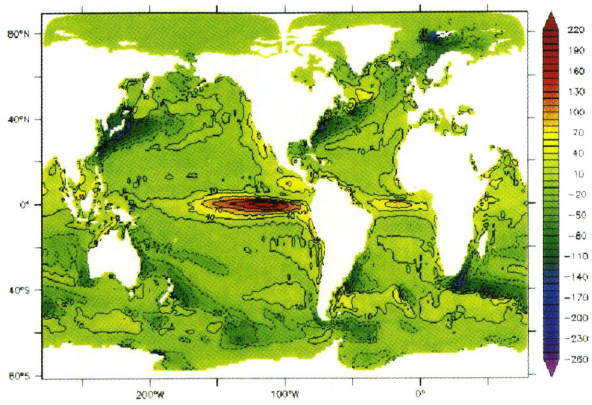

Fig 3 The annual mean surface net heat flux estimated from GCM_1

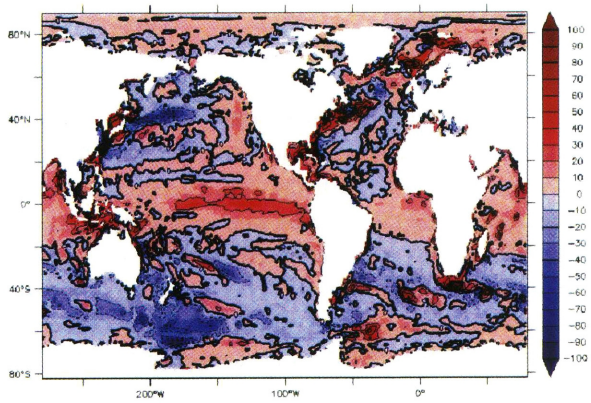

Fig. 4 Difference of the annual mean surface net heat flux between GCM_0.5 and GCM_1 (GCM_0.5 minus GCM_1)

Fig. 1 shows the difference between annual mean SST of GCM_1 and climatological SST (GCM_1 minus observation). Spatial pattern of annual mean SST bias in each hemisphere is similar to its hemispheric winter pattern in general; February in the northern hemisphere and August in the southern hemisphere. It is noted that from the equatorial Western Pacific to the Kuroshio region and along the subtropical gyre warm bias up to 2°C appears prominently. This warm bias also appears at the various regions in the southern hemisphere, ie, central part of the South Pacific (20-50°S), west coast of South America, west coast of Africa to east coast of South America in the South Atlantic, east coast of Africa to west coast of Australia in the South Indian Ocean. Central part of the Arctic Ocean (less than 0.5°C) and the regions at 140°W and 50°W along 60°S (max. 3°C) also show warm bias.

Meanwhile, cold bias also appears in various regions. Central part of the subtropical gyre, west coast of North America and the cold tongue area in the equatorial region are remarkable. Most of the North Atlantic and subarctic ocean show cold bias. Especially in the Gulf Stream region and southwest off Greenland strong cold bias of -3°C is formed. In the southern hemisphere east coast of Australia and the several places along the coast of the Antarctic continent show weak cold bias of -1 ~ -2°C.

Fig. 2 shows the difference of annual mean SST between GCM_0.5 and GCM_1. Compared with Fig.1 a large portion of warm bias region seen in GCM_1 is cooled in GCM_0.5; warm pool region in the equatorial Western Pacific, Kuroshio region along the East China Sea shelf, and southeast off Japan, East/Japan Sea, west coasts of South America and Africa, the West Indian Ocean, the Arctic Ocean and the eastern part off the Antarctic peninsula including Weddell Sea. On the other hand, a large part of the region which is colder than the observation in GCM_1 is now warmed in GCM_0.5. Among those regions the notable places are from the southeast coast of Australia to the region near to the Ross Sea, western part of the Antarctic peninsula, the central North Atlantic Ocean and the central South Atlantic Ocean.

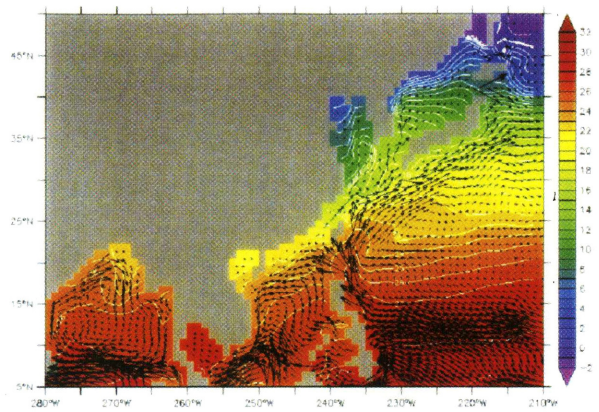

Fig. 5 Distributions of the current and the temperature field (color) in February (GCM_1)

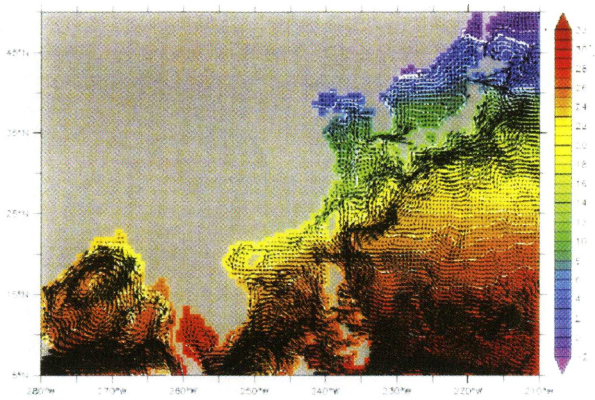

Fig. 6 Distributions of the current and the temperature field (color) in February (GCM_0.5)

• Global distribution of air-sea heat flux

Heat exchange between atmosphere and ocean determines SST and plays an important role for the formation of water mass. In the CORE experiments, it is recommend to use the common atmospheric state dataset and bulk formula for the intercomparison of various global coupled ocean-sea ice models. Actual atmosphere-ocean heat flux estimated in the model is significantly affected by the prognostic model SST.

Fig. 3 and Fig. 4 show annual mean sea surface net heat flux estimated from GCM_1 and difference of the two surface net heat flux between GCM_1 and GCM_0.5 (GCM_0.5 minus GCM_1), respectively. Equatorial Western Pacific and Indonesian archipelago region receive more heat in GCM_0.5 than GCM_1, and the East Asian Marginal Seas and the Kuroshio region south of Japan show less heat loss through the sea surface in GCM_0.5 than GCM_1. Cold tongue area in the equatorial Pacific receives more heat in GCM_0.5. In Fig. 4, the regions showing the positive difference of heat flux mostly correspond to the places where GCM_0.5 shows lower SST compared to GCM_1. On the contrary, the places showing the negative value in the heat flux difference coincide with the places where GCM_0.5 simulates higher SST than GCM_1.

Comparing Fig. 2 with Fig. 4, one can raise a question that why GCM_0.5 simulates lower SST than GCM_1 whereas it receives more heat through the surface in the areas such as the equatorial Western Pacific or the East Asian Marginal Seas? To answer this question, first we should remind the fact that in these simulations SST and heat flux distributions reached a quasi-steady state, so the year to year variation of net heat flux is almost zero. As a result the maintenance of lower SST in those areas despite of the continuous supply of heat (or less heat loss) through the surface in GCM_0.5 suggests that the heat supply in the upper layer through the heat advection and diffusion process is simulated to be smaller in GCM_0.5 than GCM_1. In other words, lesser amount of heat transport in GCM_0.5 simulates lower temperature in the surface layer, which induces relatively more heat input (or lesser heat loss) through the surface in the estimation of surface heat flux using the bulk formula.

• Global distribution of current

As the ocean-sea ice model used in this study is not a fully coupled atmosphere-ocean model, model SST is forced by the thermal forcing specified by the fixed atmospheric climatology with bulk formula and cannot change the atmospheric state interactively. Therefore, spatio-temporal variation of model SST in the steady state shows closer relation with the current field in the ocean and the surface heat flux is dependent on the SST change. In Fig. 5 and Fig. 6 current distribution is shown together with the temperature field in the Northwestern Pacific and the northeastern part of the Indian Ocean. In GCM_1 (Fig. 5), the North Equatorial Current and the Kuroshio are simulated to be broad and a rather simple flow pattern flowing westward and northeastward, respectively. Compared to it, flows in the East Asian Marginal Seas appear to be weak both in their magnitude and pattern.

However, in GCM_0.5 (Fig. 6) the Kuroshio shows narrower and more dynamic flow pattern including recirculating eddy and more meso-scale eddies in 15-30°N. The North Equatorial Current also reveals a more complex meridional structure in 5-15°N. Currents in the Yellow sea, the East China Sea and the South China Sea also show more complex, stronger and clearer flow pattern. The existence of eddy in the Bay of Bengal is clearly identified. Current system in the East Asian

Marginal Seas and the Kuroshio region simulated in detail in GCM_0.5 resolves the existence of coastal currents which transport the relatively cold water residing in the coastal area, thus makes it possible to simulate the colder SST distribution compared to GCM_1.

4. Discussion and Summary

In this study performance of SST simulation is compared with the use of global coupled ocean-sea ice model in accordance with the increase of horizontal grid resolution. The two models employed in the experiments take the same configuration and the common forcing dataset except the increased horizontal resolution and the corresponding more realistic representation of bottom topography. Simulated result exhibits the appearance of significant change in the distributions of SST and heat flux when the grid resolution moves from one degree grid spacing into 0.5 degree grid spacing (except equatorial region); going into higher resolution, coastal currents in the continental coast are simulated in more detail and contribute to the formation of low temperature area by transporting a relatively cold coastal water. In addition, the higher resolution of the model contributes to specify the heat transport and its spatial extent properly through more realistic simulation of the Western Boundary Current such as the Kuroshio in its width and spatial variations.

Comparing SST distributions in the Gulf Stream and Greenland-Iceland Sea region with the climatological SST, both GCM_1 and GCM_0.5 show cold bias more than 3℃ (Fig. 1 and Fig. 2). This area corresponds to the deep water formation region. Sea ice formation and fresh water input by the ice melting together with the heat and salt transport by the Gulf Stream play an important role for the realistic simulation of surface water properties. The effect of sea ice formation and melting for the cold bias in the north of North Atlantic and the Greenland-Iceland Sea area needs to be considered in more detail in the future.

In this global ocean-sea ice experiment the surface heat flux is demonstrated to be driven by the SST variation. This point can be understood from the bulk formula employed in the model; latent heat, sensible heat and longwave radiation are all given as a function of SST except shortwave radiation[8]. And atmospheric state variables for the estimation of thermal forcing are all given as climatologies in the model. Therefore surface heat flux difference between GCM_1 and GCM_0.5 is directly related with the prognostic model SST difference.

So far, one degree grid resolution adopted in many climate experiments meets to simulate the behavior of basin-scale boundary currents and the large scale circulation in a global perspective. However, to simulate the regional scale variability and its sea water property together with the large scale circulation, it is suggested that the horizontal resolution of a global ocean-sea ice model should be enhanced at least less than 0.5 degree grid spacing at mid-latitude which could resolve the current system in the marginal seas and meso-scale eddies.

Acknowledgments

This research was supported by the Ministry of Land, Transport and Maritime Affairs (PM56990) and the Korea Institute of Ocean Science & Technology (PE98731).

References

1) S.M. Griffies, A. Biastoch, C. Boning, F. Bryan, G. Danabasoglu, E.P. Chassignet, M.H. England, R. Gerdes, H. Haak, R.W. Hallberg, W. Hazeleger, J. Jungclaus, W.G. Large, G. Madec, A. Pirani, B.L. Samuels, M. Scheinert, A.S. Gupta, C.A. Severijns, H.L. Simmons, A.M. Treguier, M. Winton, S. Yeager and J. Yin, Ocean Model. 1-46(2009)26.
2) A.J. Semtner and R.M. Chervin, J. Geophys. Res. 5493-5550(1992)97.
3) D. Stammer, R. Tokmakian, A. Semtner, and C. Wunsch, J. Geophys. Res. 25779-25811(1996)101.
4) A.S. Gupta and M.H. England, J. Phys. Oceanogr. 2592-2614(2004)34.
5) C.J. Jang, H.S. Min, C-H. Kim, S.K. Kang, and H-J. Lie, Ocean & Polar Res. 245-258(2006)28.
6) S.M. Griffies, GFDL Ocean Group Technical Report No.6. NOAA/Geophysical Fluid Dynamics Laboratory, Princeton, USA. 444p(2009).
7) S. Levitus and coauthors, NOAA Atlas NESDIS 18, NOAA/NESDIS, U.S. Dept. of Commerce, Washington, D.C. (1998).
8) W. Large and S. Yeager, NCAR Technical Note: NCAR/TN-460+STR. CGD Division of the National Center for Atmospheric Research. (2004).
9) W.G. Large and S.G. Yeager, Clim. Dyn. 341-364(2009)33.
10) R.W. Reynolds, N. Rayner, T.M. Smith, D. Stokes, W. Wang, J. Clim. 1609-1625(2002)15.